Int. J. Multiphase Flow Vol. 12, No. 2, pp. 219–236, 1986
Printed in Great Britain.

0301–9322/86 $3.00 + .00

TWO-PHASE FLOW PATTERNS AND VOID FRACTIONS IN DOWNWARD FLOW. PART II: VOID FRACTIONS AND TRANSIENT FLOW PATTERNS

T. J. CRAWFORD† and C. B. WEINBERGER
Drexel University, Philadelphia, PA 19104, U.S.A.

and

J. WEISMAN
University of Cincinnati, Cincinnati, OH 45221, U.S.A.

(*Received* 18 *October* 1984; *in revised form* 6 *May* 1985)

Abstract—The relationship between void fraction and quality was determined as a function of mass velocity for refrigerant 113 and its vapor in steady-state downward flow. These data were used together with the so-called "dynamic slip" model to determine the product of interfacial drag, C_{LG}, and interfacial area per unit volume, A_{LG}. Visual observations of flow-pattern transitions along with drag disk and void fraction measurements, were made during flow transients. The "dynamic slip" model and the previously calculated values of $C_{LG}A_{LG}$, were used to determine the appropriate relationship between α and x during the transient. This enables comparison of the transient flow pattern observations with steady-state flow maps. The comparison indicated that the transient data approximately followed the steady-state map but that in most cases the existing flow pattern persists slightly past the steady-state boundary.

INTRODUCTION

Two-phase (gas–liquid) flow patterns during steady state were examined in part I of this paper (Crawford *et al.* 1985). Experiments using refrigerant 113 and its vapor in the University of Cincinnati's boiling refrigerant loop were reported upon there. Steady-state data were obtained in both vertically downward lines and lines declined at several angles. These data, and data from the literature, were compared with available flow maps and models. It was found that the simple flow map originally presented by Weisman & Kang (1981) could be used for downward flow providing a revised set of correction factors were used for the bubble-intermittent transition. Both the dispersed and annular flow transitions appeared essentially unchanged. In the present paper, flow pattern behavior during downward flow transients is examined. Void fraction behavior and its relationship to flow patterns is also considered.

Previous transient studies

The limited experimental data in the literature appear to deal exclusively with air–water behavior in horizontal flow. Sakaguchi *et al.* (1976,1979) examined behavior in transients induced by a step change in air or water flow rates in horizontal lines. They noted the occurrence of a temporary intermediate flow pattern (slug or waves) during a transient period between the initial and final steady-state flow patterns. These intermediate flow patterns were only seen with large air flow rate changes; no such intermediate patterns were seen with small airflow rate changes or any size water flow rate change.

Taitel *et al.* (1978) also examined air–water flow in horizontal lines. These investigators primarily examined flow transients originating in the stratified or wavy regions. They also noted that, during very rapid gas flow rate increases, flow patterns which would not be expected for slowly changing flows occured during the course of the transient. No such unexpected flow patterns were seen in liquid flow rate ramps. However, in both types of ramps they observed flow pattern transition locations which often differed from those of steady-state.

Taitel *et al.* (1978) developed a theoretical analysis based on the application of mass and momentum conservative equations to the initial stratified-flow geometry. Predictions

† Present Address, American Electric Power, Columbus, OH 43215.

of the liquid velocity and height were obtained as a function of time and distance along the pipe.

The theoretical work of Mishima & Ishi (1984) is probably more readily applicable to the current computational procedures used for examining two-phase flow transients in large systems. In particular, the computer programs developed for the analysis of hypothetical accidents in nuclear reactors rely on the use of a general set of mass, momentum and energy conservation equations. The more advanced of these programs write separate conservation equations for each phase and require additional constitutive equations specifying the interfacial transfer rates. Mishima & Ishi (1984) have proposed models for these interfacial transfer rates which depend on the flow pattern present. This obviously requires that the designer be able to predict the flow pattern.

Mishima & Ishi (1984) have also proposed criteria for the various flow pattern transitions. They consider the usual criteria given in terms of superficial velocities to be unsuitable for use during transients. Under steady state conditions, a given set of gas and liquid superficial velocities specifies the void fraction. Mishima & Ishi (1984) note that in a rapid transient this will not be true since α will depend partly on a previous history. They believe that the void fraction presents the major factor in determining the flow pattern. Their flow pattern transition criteria are therefore primarily based on void fraction relationships.

A somewhat similar idea is presented by Kaizerman *et al.* (1983). They also note that the transient α at given superficial gas and liquid velocities may not correspond to the steady-state value. They therefore suggest that the flow pattern map be expressed in terms of a total mixture velocity and α. They suggest that, for a given system, such a map would apply, during transients at any pressure.

McFadden *et al.*'s (1981) approach in their version of the RETRAN code follows a closely related path. They use the Bennett *et al.* (1965) flow map, which is based on G vs α coordinates, and take the map to be independent of pressure.

Approach of present investigation

In the present study, flow pattern transition observations were made during a series of flow transients. The transient observations were then compared to the steady-state results described in part I of this paper.

The experimental technique used in the transient studies required that the relationship between x and α be known during the transient. Therefore, prior to studying flow pattern behavior during flow transients, the steady-state relationship between α and x was determined. Available theory was then used to determine the α-x relation which could be used during the transients.

Void fraction studies

The void fraction measurements with vertically downward flow of refrigerant 113 were obtained using the University of Cincinnati's boiling freon loop. The loop arrangement used for these tests has been described in part I of this paper (Crawford *et al.* 1985). The two-phase mixture, provided by upstream electrical heaters, flowed downstream through a 2.5-cm diameter, 1.5-m-long glass test section.† The total of the test-section flow and mass flux, G, was determined by an orifice meter placed in the single phase region upstream of the heater. The two-phase mixture quality was obtained from G and the reading of a drag disk placed at the test section exit. The drag disk, which was a perforated disk covering the entire flow area, was preceded by a homogenizing screen. Previous studies (Weisman 1977) had shown that the reading of such a drag disk was proportional to G^2/ρ_{hom} where ρ_{hom} is the density of a homogeneous mixture of the same quality.

The void fraction in the test section was obtained from the reading of a D/P cell connected across the test section. After appropriate correction of the D/P cell reading for friction losses, which were small, the elevation head provided the mean void fraction. The procedure is very simple and convenient to use for vertical pipe lines. Previous studies by Tentner (1977) have shown this approach to agree well with void fractions determined by

† The loop configuration used for the void fraction studies differed only slightly from that used for the transient studies and shown in figure 6.

a capacitance type sensor even in the annular flow region. More recently, comparisons with gamma densitometer measurements at the University of Cincinnati have shown good agreement through all of the flow patterns observed in vertical flow.

Data were taken at 2 bar and 4 bar (absolute) in both a 2.5- and 3.8-cm diameter lines. Typical data at 2 bar for D = 2.5 cm are shown in figure 1. The horizontal and vertical bars drawn through some of the points provide an estimate of the 2σ error range in α and x. It will be observed, as may be expected for downward flow, that the slip ratios are below 1.0. Further, there is a strong velocity effect; the data at higher velocities having gas–liquid velocity ratios closer to 1.0. Tube diameter, appeared to have no effect over the limited range examined.

On the basis of figure 1, and similar figures for the other conditions tested, a set of smoothed curves of α vs x, as a function of G, was prepared for each of the two pressures examined. The set of smoothed curves for $P \simeq 2$ bar is shown in figure 2. The smoothed data were first compared to Petrick's (1963) velocity ratio correlation for downward flow, but poor agreement was found. Considerably better agreement could be obtained with the

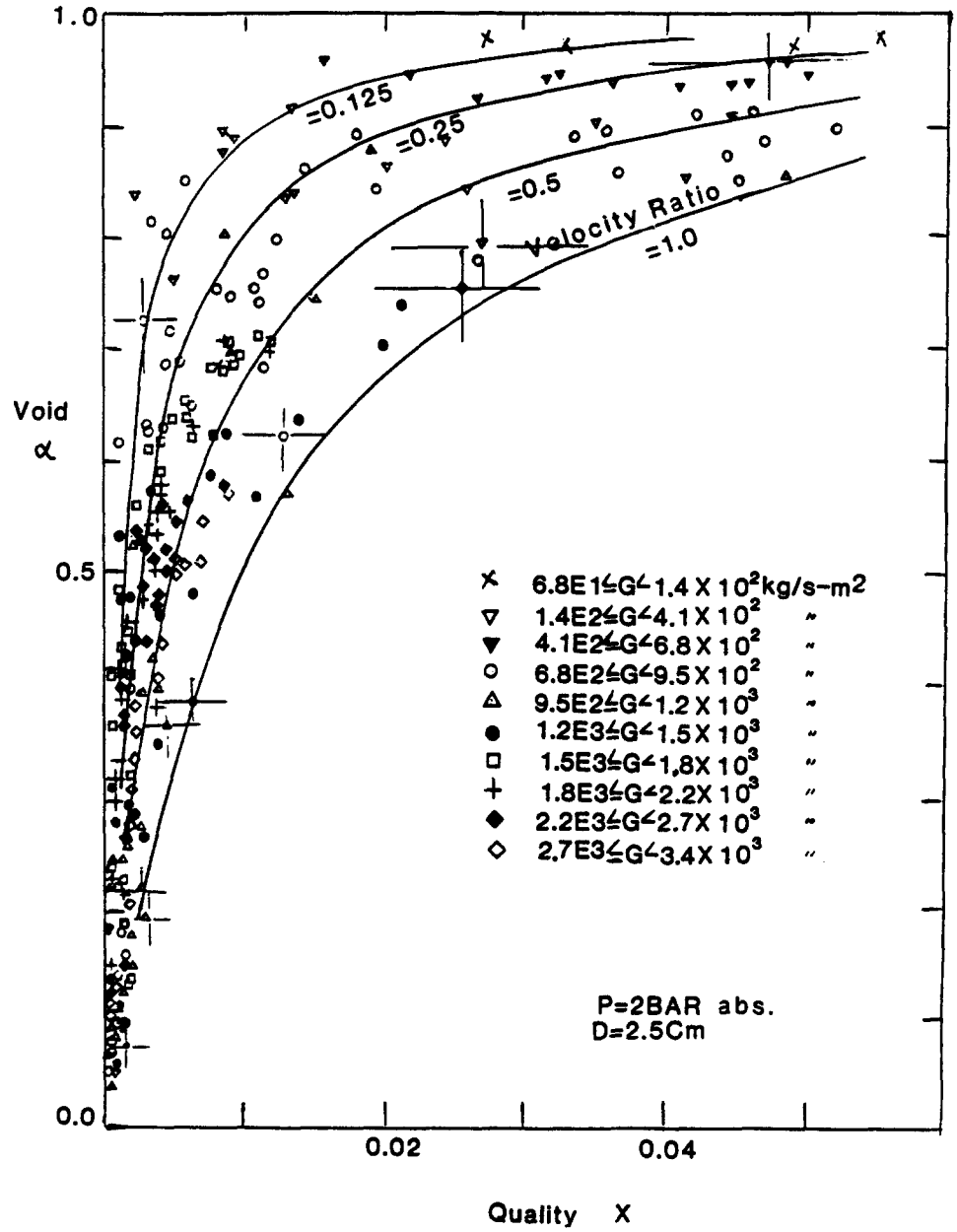

Figure 1. Typical void fraction data at 2 bar (D = 2.5 cm).

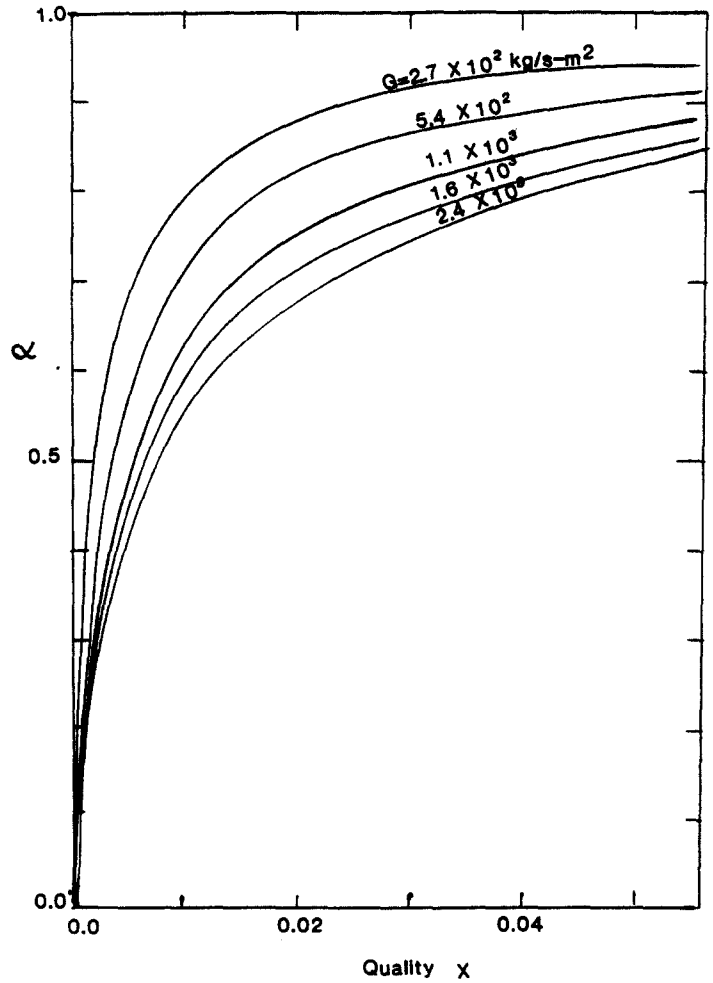

Figure 2. Void vs quality relationship as a function of G (P = 2 bar).

drift flux model of Zuber & Findlay (1965). With this model the relationship between average void fraction, α, and quality, x, is written as

$$\alpha = \frac{x/\rho_G}{C_0[x/\rho_G + (1-x)/\rho_L] + V_{gj}/G} \quad , \qquad [1]$$

where C_o = distribution parameter, dimensionless and ρ_G, ρ_L = gas and liquid densities, respectively (mass/volume). The distribution parameter, C_o, is determined by the vapor velocity and concentration profiles across the channel. The mean drift velocity V_{gj}, represents the difference between the gas phase velocity and the average mixture velocity. For vertical upward flow, Lahey & Moody (1977) assume that the drift velocity may be set at the bubble rise velocity and taken as independent of flow pattern. This suggestion is followed here and V_{gj} is taken as the plug or cap bubble velocity recommended by Collier (1981). For downward flow,

$$V_{gj} = -0.35\,[g(\rho_L-\rho_G)D/\rho_L]^{1/2} \quad , \qquad [2]$$

where g = acceleration due to gravity (length/time^2). The value of C_o required to fit the data depended on both the flow pattern and pressure. The values found most appropriate are listed in table 1. It will be noted that all the tabulated values of C_o are 1.0 or lower which is in contrast to the values commonly employed in upward flow where $C_o \geq 1.0$. According to Zuber & Findlay (1965) values greater than one generally indicate the vapor is being transported more rapidly than the average flow velocity. Since in downward flow

Table 1. Value of C_0 for drift flux model with downward flow of refrigerant 113

Pressure	Flow Pattern Bubble	Intermittent	Annular
2 bar	0.8	0.95	1.0
4 bar	0.85	0.9	1.0

the vapor is transported more slowly than the average flow, values of $C_0 \leq 1.0$ seem reasonable. Note that although $C_0 = 1$ for annular flow, this does not mean that the vapor and liquid have the same velocity since V_{gj} is not zero.

Although the use of [1] requires a knowledge of the flow pattern in order to select appropriate values of C_0 and V_{gj}, this causes no difficulty. The flow pattern map presented in part I of this paper (Crawford *et al.* 1985) requires only a knowledge of x, mass flux and fluid properties.

More germaine to the present study than the drift flux model is the so-called "dynamic slip" approach of McFadden *et al.* (1981). In the latter approach, transient two-phase flows are described in terms of four differential equations. These are the continuity, momentum and energy equations for the mixture and one equation describing the dynamic behavior of the phase velocity difference ("dynamic slip" equation). The "dynamic slip" equation is derived by first writing the momentum equations for the vapor and liquid phases in convenient form, subtracting the resultant equations and solving for the time derivative of the relative velocity. On obtains

$$\frac{\partial V_{LG}}{\partial t}\left(1+\frac{A_m\bar{\rho}}{\alpha(1-\alpha)\rho_{LG}\rho_g}\right) = -\left(\frac{1}{\rho_L}-\frac{1}{\rho_G}\right)\frac{\partial P}{\partial z} - \frac{\bar{\rho}A_{fg}B_{LG}V_{LG}}{\alpha(1-\alpha)\rho_L\rho_G} + V_G\frac{\partial V_G}{\partial z} - V_L\frac{\partial V_L}{\partial z} + \frac{A_{wG}B_{wG}V_G}{\alpha\rho_G} - \frac{A_{wL}B_{wL}V_L}{(1-\alpha)\rho_L} \quad , \quad [3]$$

where A_{LG} = interfacial (liquid–gas) surface area per unit volume, (length)$^{-1}$, A_m = added mass coefficient, A_{wA} = surface area of phase "a" per unit volume in contact with wall, (length)$^{-1}$, B_{LG} = friction coefficient between gas phase and liquid phase, B_{wa} = drag between wall and phase "a", P = pressure (force/area), t = time, V_L,V_G = liquid and gas velocities, respectively (length/time), V_{LG} = relative velocity = $V_L - V_G$ (in downward flow), z = axial distance (length), $\bar{\rho}$ = average density of mixture (mass/volume) and other symbols have their previous meaning. Further simplification is achieved by noting that, for all flow patterns seen during both steady-state and transients in vertical lines, only the liquid was in contact with the wall. Therefore, the term containing friction between vapor and wall was set to zero. When the wall–gas contact area (A_{wG}) is set to zero, the liquid area in contact with the wall per unit volume is then $4/D$, where D is the pipe diameter. We then have

$$\frac{\partial V_{LG}}{\partial t}\left(1+\frac{A_m\bar{\rho}}{\alpha(1-\alpha)\rho_L\rho_G}\right) = -\left(\frac{1}{\rho_L}-\frac{1}{\rho_G}\right)\frac{\partial P}{\partial z} - \frac{\bar{\rho}A_{LG}B_{LG}V_{LG}}{\alpha(1-\alpha)\rho_L\rho_G} + \frac{V_G\partial V_G}{\partial z} - \frac{V_L\partial V_z}{\partial z} - \frac{(4/D)B_{wL}V_L}{(1-\alpha)\rho_L} \quad . \quad [4]$$

Further simplification of [4] may be accomplished by examining the magnitude of the various terms. It is found that the terms $\frac{V_G\partial V_G}{\partial z}$ and $\frac{V_L\partial V_L}{\partial z}$ are both negligible with respect to the other terms even for very rapid flow transients in the absence of heating. The resulting equation is then

$$\frac{\partial V_{LG}}{\partial t}\left(1+\frac{A_m\bar{\rho}}{\alpha(1-\alpha)\rho_L\rho_G}\right) = -\left(\frac{1}{\rho_L}-\frac{1}{\rho_G}\right)\frac{\partial P}{\partial z} - \frac{\bar{\rho}A_{LG}B_{LG}V_{LG}}{\alpha(1-\alpha)\rho_L\rho_G} - \frac{(4/D)B_{wL}V_L}{(1-\alpha)\rho_L} \quad . \quad [5]$$

The relative velocity can be computed from [5] if (a) the product of the frictional coefficient and interfacial area per unit volume ($A_{LG}B_{LG}$) is known and (b) the added mass coefficient A_m, is known. McFadden *et al.* (1981) expressed A_m as

$$A_m = c(1-\alpha)(\alpha)\bar{\rho} \qquad [6]$$

where

$$c = (0.5+\alpha)/(1-\alpha), \qquad \alpha \leqslant 0.5,$$
$$c = (1.5/\alpha) - 1, \qquad \alpha \geqslant 0.5.$$

The $A_{LG}B_{LG}$ term was evaluated on the basis of mechanistic models for the various flow patterns. Alternatively, we may evaluate the interfacial friction term from steady-state, adiabatic quality vs void data.

At steady-state, we set $\partial V_{LG}/\partial t = 0$ in [4]. In addition, B_{LG} is replaced in terms of an interfacial drag coefficient C_{LG} and B_{wL} in terms of the liquid phase friction. That is

$$B_{LG} = C_{LG}(\tfrac{1}{8}\rho_L V_{LG}),$$
$$A_{wL}B_{wL} = (4/D)(\tfrac{1}{8}\rho_L V_L f). \qquad [7]$$

Where f = single phase D'Arcy friction factor (dimensionless). We then have

$$0 = -\left[\frac{1}{\rho_L} - \frac{1}{\rho_G}\right]\frac{\partial P}{\partial z} - \frac{A_{LG}C_{LG}\tfrac{1}{8}\rho_L V_{LG}^2)\bar{\rho}}{\alpha(1-\alpha)\rho_L\rho_G} - \frac{(4/D)(\tfrac{1}{8}\rho_L V_L f)V_L}{(1-\alpha)\rho_L} \quad . \qquad [8]$$

A working form of the foregoing equation is obtained by (a) replacing V_L and V_{LG} in terms of x, and α, and G and (b) expanding dP/dz in terms of its components.

The velocities V_L and V_{LG} are written as

$$V_L = \frac{G(1-x)}{\rho_L(1-\alpha)} \quad , \qquad [9]$$

$$V_{LG} = G\left(\frac{1-\alpha}{\rho_L(1-\alpha)} - \frac{x}{\alpha\rho_G}\right) \quad . \qquad [10]$$

The pressure drop is written in terms of the friction and elevation components only since it is found that, in the absence of heating, the acceleration component is negligible. We then have

$$\left(\frac{1}{\rho_L} - \frac{1}{\rho_G}\right)\frac{dp}{dz} = \left(\frac{\Delta\rho}{\rho_L\rho_G}\right)\left(\frac{\bar{R}fG^2}{2D\rho_L} - \bar{\rho}g\right) \quad , \qquad [11]$$

where $\bar{R}$ = two-phase friction multiplier, dimensionless

$$\Delta\rho = \rho_L - \rho_G.$$

After making the foregoing substitutes, rearranging terms and solving for $A_{LG}C_{LG}$, it is found that

$$A_{LG}C_{LG} = \left[\frac{-f}{2D\rho_L^2}\left(\frac{\bar{R}\Delta\rho}{\rho_G} + \frac{(1-x)^2}{(1-\alpha)^3}\right) + \frac{\bar{\rho}g\Delta\rho}{G^2\rho_G\rho_L}\right]\frac{8[\alpha(1-\alpha)\rho_G\rho_L]^3}{[(1-x)\alpha\rho_G - x(1-\alpha)\rho_L]^2\bar{\rho}\rho_L^2} \quad . \qquad [12]$$

It should be noted that in expressing the interfacial friction solely in terms of an interfacial

drag coefficient we are ignoring turbulent shearing stress which are not dependent of the difference in phase velocities. The present model thus fails when one gets to fully dispersed flow where V_{LG} approaches zero. Since one would expect the turbulent shearing stresses to vary with $(G/\bar{\rho})^{1.8}$, the correction will only be important as the mass velocity approaches 10×10^6 kg/h m^2 (onset of dispersed flow).

Figure 3 shows the smoothed values of $A_{LG}C_{LG}$ obtained from the void-quality curves at 2 bar (curves of figure 2) by application of equation [12]. The values of $A_{LG}C_{LG}$ are plotted vs α with total mass velocity, G, as a parameter. The symbols shown on the curves are only being used to identify the mass velocity at which the given curve was obtained. It may be seen that there is a marked velocity dependence with the interfacial drag decreasing as the mass velocity increases. Since a correction for the turbulent shearing stresses was not included, curves for values of G above 6×10^6 kg/h m^2 are not shown. At lower G values, the correction is not significant.

All of the curves in figure 3 have the same general shape. The values of $A_{LG}C_{LG}$ increase with α at low voids (bubbly region) but decrease with α at intermediate and high voids (intermittent and annular regions). Once curves of $A_{LG}C_{LG}$ have been obtained from analysis of the experimental data these curves may be used to calculate α for a given x and G. This is accomplished by use of [8] together with an iterative solution procedure.

It is of interest to compare the values of α predicted by the various models with observations. A typical comparison is shown in figure 4 where we plot the difference between prediction and observation, $(\Delta\alpha)$ against quality, x, for a mass velocity of 2×10^6 kg/m^2 h at P $\simeq$ 2 bar. The drift flux model provides reasonable agreement and the "dynamic slip" model is most accurate.

Flow pattern transition maps in terms of G and α

It has been noted previously that McFadden *et al.*'s (1983) version of RETRAN used a flow map based on G vs α . In figure 5 we have used this approach and plotted the observed steady-state flow pattern transition lines in G vs α coordinates for both 2- and 4-bar observations. The void fraction values are based on the observed empirical relationship between α and x.

It may be seen in figure 5 that generally good agreement is obtained between the data at the two pressure levels investigated. Some diameter effects are still observed with the 3.8-cm-line data being somewhat above the 2.5-cm-line data for both the bubble-intermittent

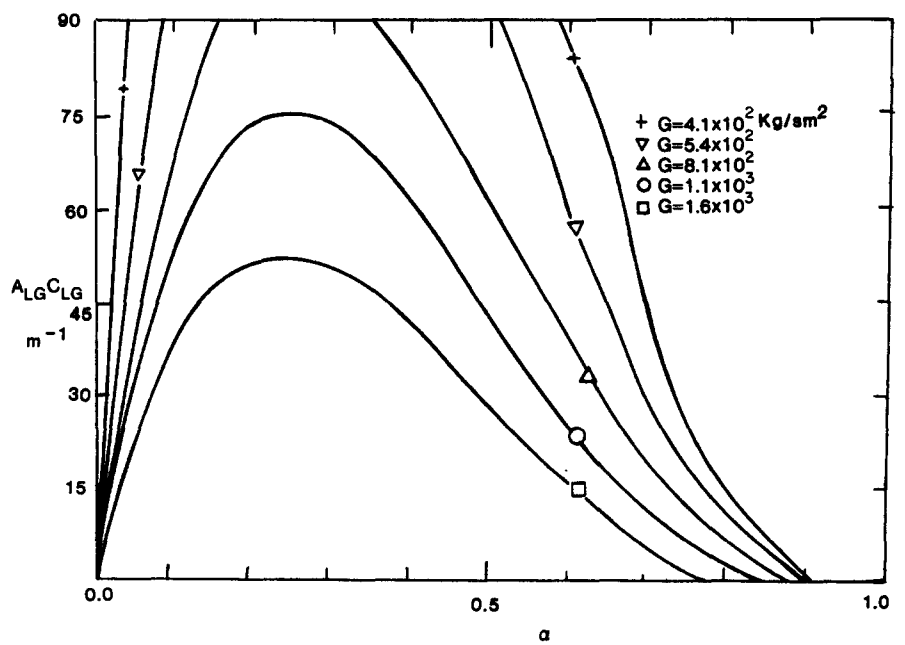

Figure 3. $A_{LG}C_{LG}$ from "dynamic slip" model for downflow of refrigerant 113 at 2 bar.

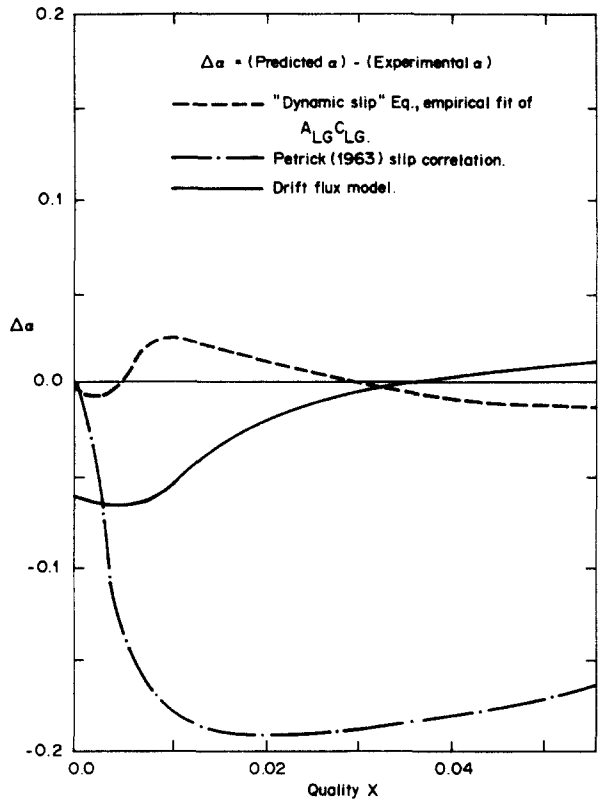

Figure 4. Comparison of model predictions of α with observations.

and annular flow transitions. This is to be expected since line diameter effects which are required for use with Weisman & Kang's (1981) superficial-velocity coordinate map are not considered here.

It will also be observed that when G vs α coordinates are used, the falling film flow pattern (separated flow) occupies a very small region. In these coordinates, this region could very easily be combined with the annular region.

Transient experiments

The boiling refrigerant loop used for flow-pattern observations during flow transients is shown in figure 6. The basic configuration is identical to that used during steady-state tests but a three-way valve was installed some distance upstream of the test section. By rapidly moving this valve a portion of the two-phase mixture could be made to bypass the test section and a flow transient produced.

The void fraction of the two-phase mixture leaving the test section was determined by a capacitance type void sensor identical to that previously used by Weisman *et al.* (1979) and Weisman & Kang (1981) for their steady-state experiments. The flow was determined from the reading of the same drag disk as used in the steady-state void fraction determination described in the preceding section of this paper. The signals from both the drag disk and void sensor were fed to separate channels of a recording oscillograph.

When the test was conducted, the experimenter visually observed the flow patterns and noted the order of their appearance. Whenever there was a change in flow pattern the experimenter pressed a hand held switch. This caused a signal to be transmitted to the oscillograph recording thus allowing the flow and void conditions at the time of the flow pattern transition to be determined.

The void sensor and drag disk were located immediately downstream of the test section as shown in figure 6. In relating the instrument readings to the visual observations, a correction was made for the time needed for the two-phase mixture to pass from the test section to the instrumentation position. These times ranged from about 0.4 sec for the slowest transients to less than 0.1 sec for the fast transients. It is recognized that this simple

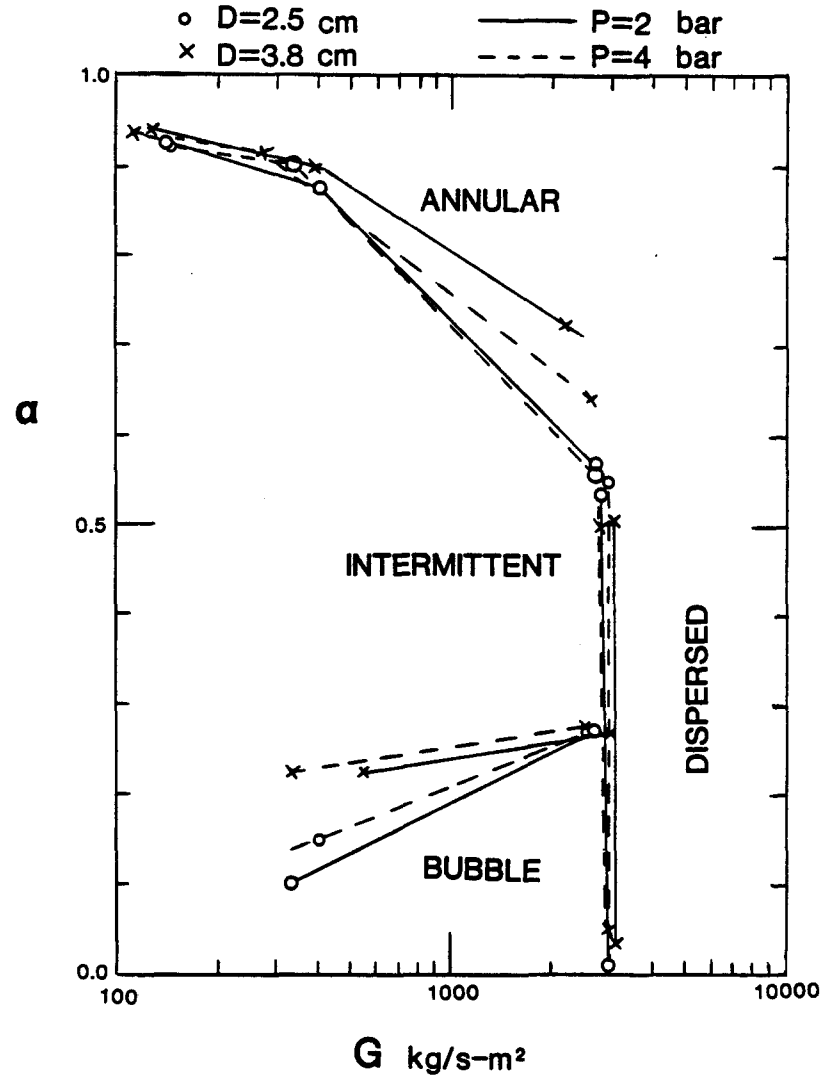

Figure 5. Comparison of flow pattern transitions at 2 bar and 4 bar.

correction is only approximate. However, it is believed that the error involved in over correcting or under correcting was small compared to instrument error, signal fluctuations, and the subjective nature of visual flow pattern observation and identification.

It has been noted previously that the drag disk signal was proportional to G^2/ρ_{hom}, and that ρ_{hom}, the homogenous density, depends on the quality, x. Unfortunately, only the void fraction, α, was available from experimental observation. Hence, x had to be determined from α. At the outset of this study it was expected that the "dynamic slip" model would be required to make this determination.

Flow transients with both increasing and decreasing flow ramps were carried out. Initial ramp rates, $(\Delta G/\Delta t)$, were of the order of 10^6 to 2.2×10^6 (kg/sec m²)/sec. These ramp rates decreased with time as the transient progressed and approached zero as the flow approached its final equilibrium value. The transients were completed in 5 to 10 sec. For the first 1 to 1.5 sec during the transient, the quality remained essentially constant since the two-phase mixture entering the test section during this period had passed through the heaters prior to the onset of the transient. Subsequently, the quality would decrease in the increasing flow transients and increase in the decreasing flow transients.

To determine the effects of the dynamic terms of the void-quality relationship, the observed void fractions were compared to those calculated by the "dynamic slip" model during the first 1 to 1.5 sec of a number of transients. In order to accomplish this, it is necessary to return to [5] and make the substitutions indicated by [6], [7], [9] and [10].

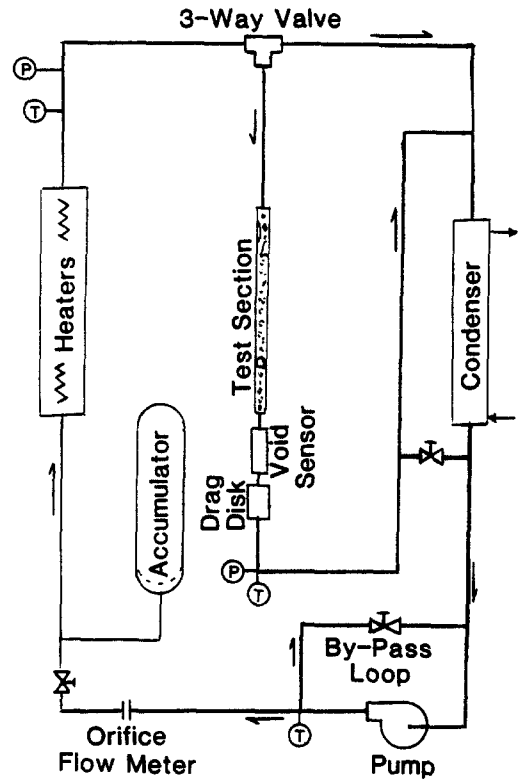

Figure 6. Loop configuration for transient tests.

With the assumption of constant x, the left-hand side of [5] then becomes

$$\frac{\partial V_{LG}}{\partial t}\left(1+\frac{A_m\bar{\rho}}{\alpha(1-\alpha)\rho_L\rho_G}\right) = \left[G\frac{d\alpha}{dt}\left(\frac{1-x}{\rho_L(1-\alpha)^2}+\frac{x}{\alpha^2\rho_G}\right)+\left(\frac{1-x}{\rho_L(1-\alpha)}-\frac{x}{\alpha\rho_G}\right)\frac{dG}{dt}\right]\cdot\left(1+\frac{c\bar{\rho}^2}{\rho_L\rho_G}\right). \quad [13]$$

The pressure drop must now include the acceleration pressure drop. If this latter quantity is expressed in terms of $\partial G/\partial t$, we have

$$\left(\frac{1}{\rho_L}-\frac{1}{\rho_G}\right)\frac{\partial\rho}{\partial z} = \left(\frac{\Delta p}{\rho_L\rho_G}\right)\left(\frac{\bar{R}fG^2}{2D\rho_L}-\bar{\rho}g+\frac{G}{\bar{\rho}a}\frac{\partial G}{\partial t}\right), \quad [14]$$

where $a = \partial z/\partial t$ = sonic velocity at given α.

It is then possible to rewrite [5] as

$$\left[G\frac{d\alpha}{dt}\left(\frac{1-x}{\rho_L(1-\alpha)^2}+\frac{x}{\alpha^2\rho_G}\right)+\left(\frac{1-x}{\rho_L(1-\alpha)}-\frac{x}{\alpha\rho_G}\right)\frac{dG}{dt}\right]\left(1+\frac{c\bar{\rho}^2}{\rho G\rho_L}\right) = -\frac{fG^2}{2D\rho_L^2}\left(\bar{R}\frac{\Delta\rho}{\rho_G}+\frac{(1-x)^2}{(1-\alpha)^3}\right)+\frac{\Delta\rho}{\rho_G\rho_L}\left(\bar{\rho}g-\frac{G}{a\bar{\rho}}\frac{dG}{dt}\right) \quad [15]$$

$$-\frac{(C_{LG}A_{LG})G^2[(1-x)\alpha\rho_G-x(1-\alpha)\rho_L]^2\bar{\rho}\rho_L}{8[\alpha(1-\alpha)\rho_L\rho_G]^3}.$$

Equation [5] may be arranged to give $d\alpha/dt$ in terms of α, x, $\bar{\rho}$, $(C_{LG}A_{LG})$, dG/dt and fluid properties. The assumption is made that A_LC_{LG} is only a function of α and G and hence the steady-state values of the parameter may be used. We may now apply a numerical

procedure (e.g., Runge–Kutta or predictor-corrector method) to calculate obtain α as a function of time for the experimental conditions of known initial conditions (α, x, G), constant x during the transient, and given dG/dt.

The experimental values needed for comparison were readily obtained from the oscillograph data. Since quality was constant during the initial period, $\bar{\rho}$ was known and the mass flow rate, and hence dG/dt, could be determined unambiguously as a function of time from the drag disk reading. As noted previously, the void fraction was obtained from the void sensor reading.

The results obtained for two typical transients are shown in figures 7 and 8. The data points shown in these figures represent readings from the recording oscillograph. The vertical and horizontal lines through the points represent estimates of the two σ errors in the values of the plotted parameters (Crawford 1983). It will be observed that the agreement between the "dynamic slip" model and the data points is good. However, more important is the observation that when the dynamic terms of the "dynamic slip" model were set to zero essentially the same void fraction prediction was obtained. This equality of the steady-state result with the dynamic calculations was obtained in all the transients examined. It was therefore concluded that the dynamic terms in the "dynamic slip" equation had no significant influence at the flow ramp rates examined in these tests.

The magnitude of the mass velocity ramp rates required to produce significant differences between steady-state and dynamic calculations may be seen in figure 9. The uppermost set of curves represent the time variation computed with both models for a typical transient at the actual ramp rate used. The computations were then repeated for a series of increasing flow ramp rates. It may be seen that flow ramp rates two orders of magnitude higher than those actually used were needed to obtain significant deviations between the steady-state and dynamic approaches.

In view of the foregoing, it was concluded that the steady-state empirical correlation would provide as good a relationship between void and quality during the transients as the "dynamic slip" model. Since the steady-state model was much simpler to apply, it was used for all transients to obtain the quality needed to get ρ_{hom} and allow G to be computed.

Flow pattern behavior during transients

The flow transient experiments conducted with fluid flowing vertically downward were conducted at both 2 bar and 4 bar. All were conducted in a 2.5-cm diameter line. The transients conducted may be divided into four categories. Three of these involved ramp flow increases while the fourth involved a decreasing flow.

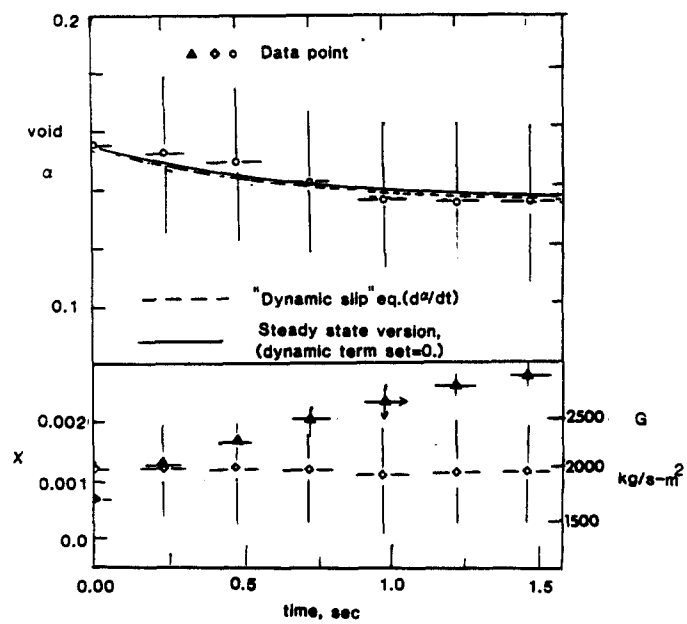

Figure 7. Comparison of "dynamic slip" equation with transient data.

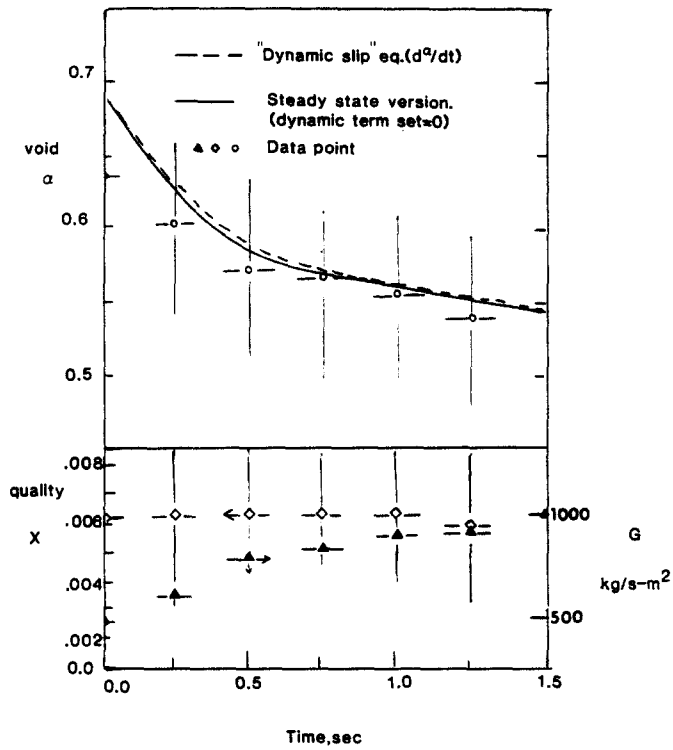

Figure 8. Comparison of "dynamic slip" equation with transient data.

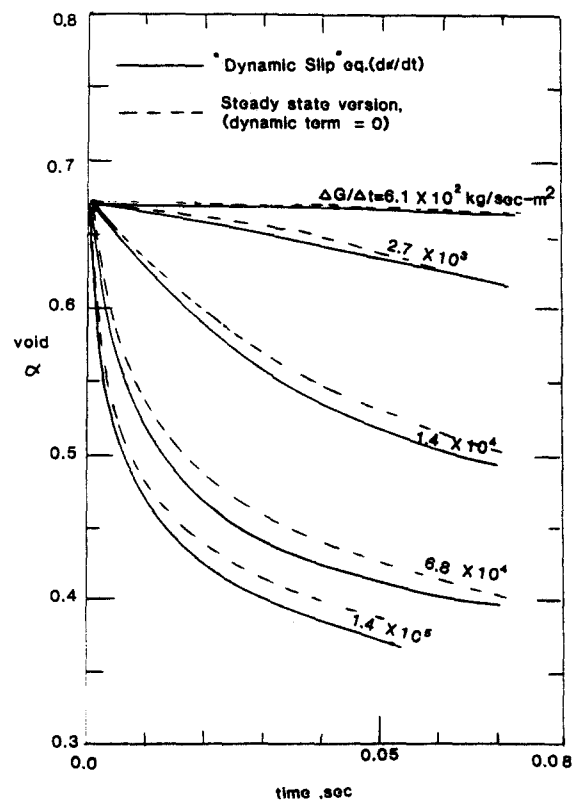

Figure 9. Effect of ramp rate on deviation of transient α from steady-state value.

The first set of increasing flow transients began in the intermittent region and progressed to the bubble or dispersed regions. For simplicity we designate these runs as $I/B/D$ transients. Figures 10(a) and 10(b) illustrate the results obtained at 2 and 4 bar on an α vs G plot. The observed steady-state transition regions are shown as shaded regions. The observations for a given run are all identified by the same number. The point at which the transient began is identified by a circle around the number. The other points represent the conditions at which a change in flow pattern was observed.

The dotted line shows the course of typical transients. The initial subflow pattern for run 6 in figure 10(a) is in the intermittent region was simiplug (see part I of this paper for flow pattern descriptions). This changed to a mixture of small plugs and bubbles, designated as the "transition" pattern, and finally to bubble. Note that although the "transition" flow pattern appears in most runs before the steady-state transition region is reached, the full bubble pattern does not actually appear in most runs until somewhat after the steady-state transition region is passed. There would thus seem to be a tendency for the intermittent region to persist for somewhat longer than would be expected on the basis of steady-state data. However, the transition to the dispersed regime takes place very close to the steady-state transition region.

The second set of increasing flow transients began in the annular or falling film regions and proceded to the intermittent, bubble and sometimes dispersed region. These transients, designated $A/I/B$, are illustrated in figures 11(a) and 11(b). Again circled numbers indicate the initial point and all other points indicate observed flow transitions. The dotted lines continue to indicate the course of typical transients.

In going from the annular and falling film region to the intermittent region, there is a tendency for the transition to be delayed beyond the steady-state transition region. This tendency is most noticeable at the lower mass flow rates. When moving into the bubble region, the "transition" subflow pattern again appears well before the steady-state transition region. As noted previously there is a tendency for the final appearance of full bubbly flow to be delayed past the steady-state transition. There is, however, no apparent delay in the transition to dispersed flow which takes place very close to the location predicted by steady-state data.

A third set of increasing flow transients were conducted in which the flow pattern changed from bubble to dispersed. In all the runs, both at 2 bar and 4 bar, the flow pattern transition occured at, or very close to, the steady state transition region.

The final set of flow transients involved decreasing flows. These transients, which went from dispersed to bubble or intermittent, were designated as $D/B/I$ transients. As may be seen from figures 12(a) and 12(b), there is again a tendency for the original flow pattern to persist beyond the region which it occupies under steady-state conditions. The disappearance of dispersed flow does not occur until a mass velocity significantly below the steady-state value is reached. While this might have been expected for the bubbly intermittent regions, it is somewhat surprising for the bubble-dispersed transition since during the increasing flow transients the transition from bubble to dispersed flow occured at the steady-state transition.

CONCLUSIONS

Consistent with the observation of other investigators (Petrick 1963; Hughmark 1962) of upward flow, the relationship between void fraction and quality in downward flow is highly dependent on mass velocity. An approximate representation of the behavior may be obtained via the drift flux model if differing values of C_0 are assigned to the various flow patterns. A more accurate representation of the steady-state data can be obtained in terms of the interfacial drag of the "dynamic slip" model. If the assumption that the product of interfacial drag coefficient and interfacial area per unit volume depends only on α and G is correct, then the "dynamic slip" model provides a means for relating α and x during transients.

The use of a flow pattern map in terms of α and G, for a given vapor–liquid system, would appear to provide a simple way of relating steady-state flow pattern transitions at

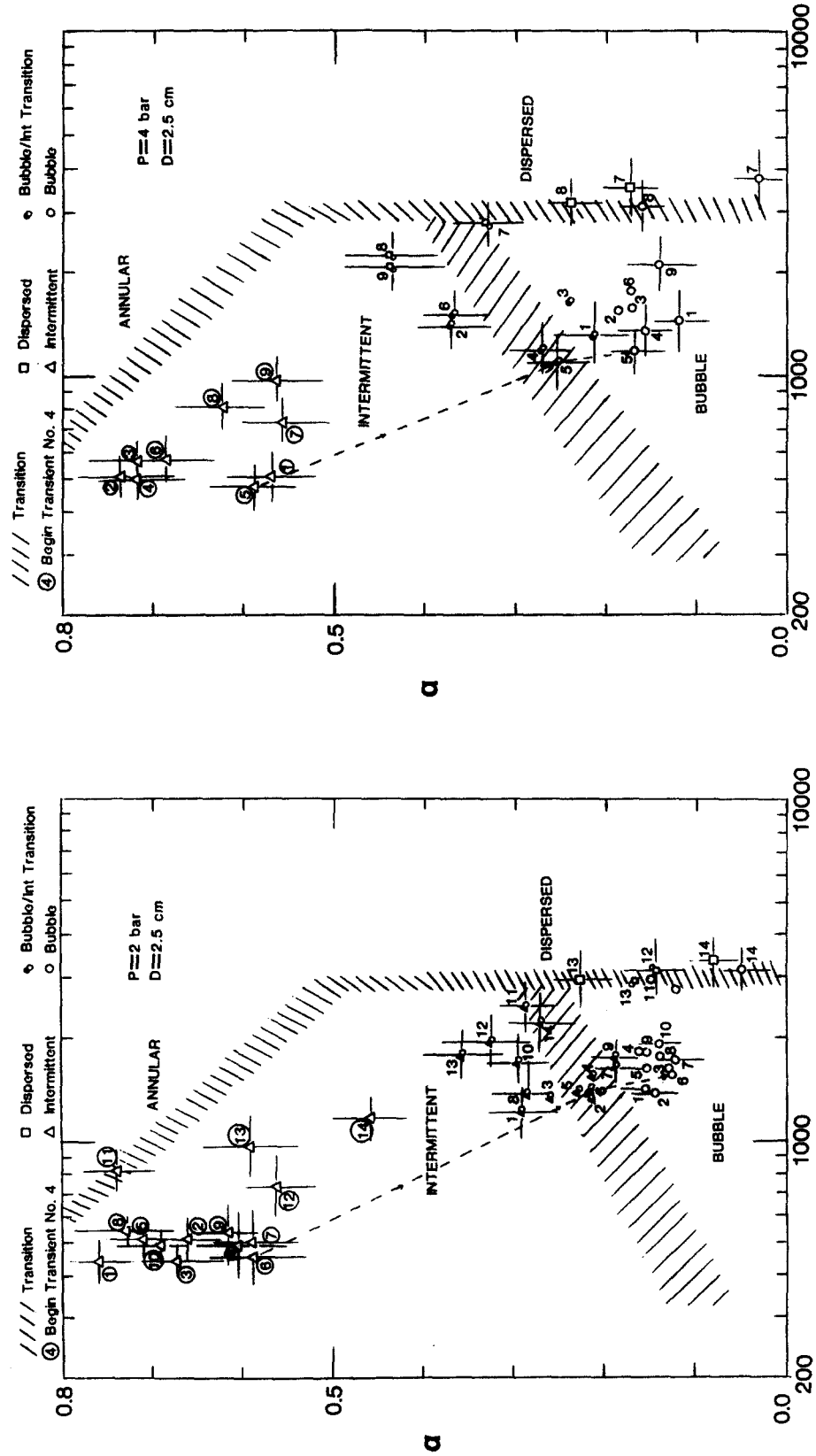

Figure 10. Intermittent/bubble/dispersed ($I/B/D$) flow transients. (a) $P = 2$ bar, (b) $P = 4$ bar.

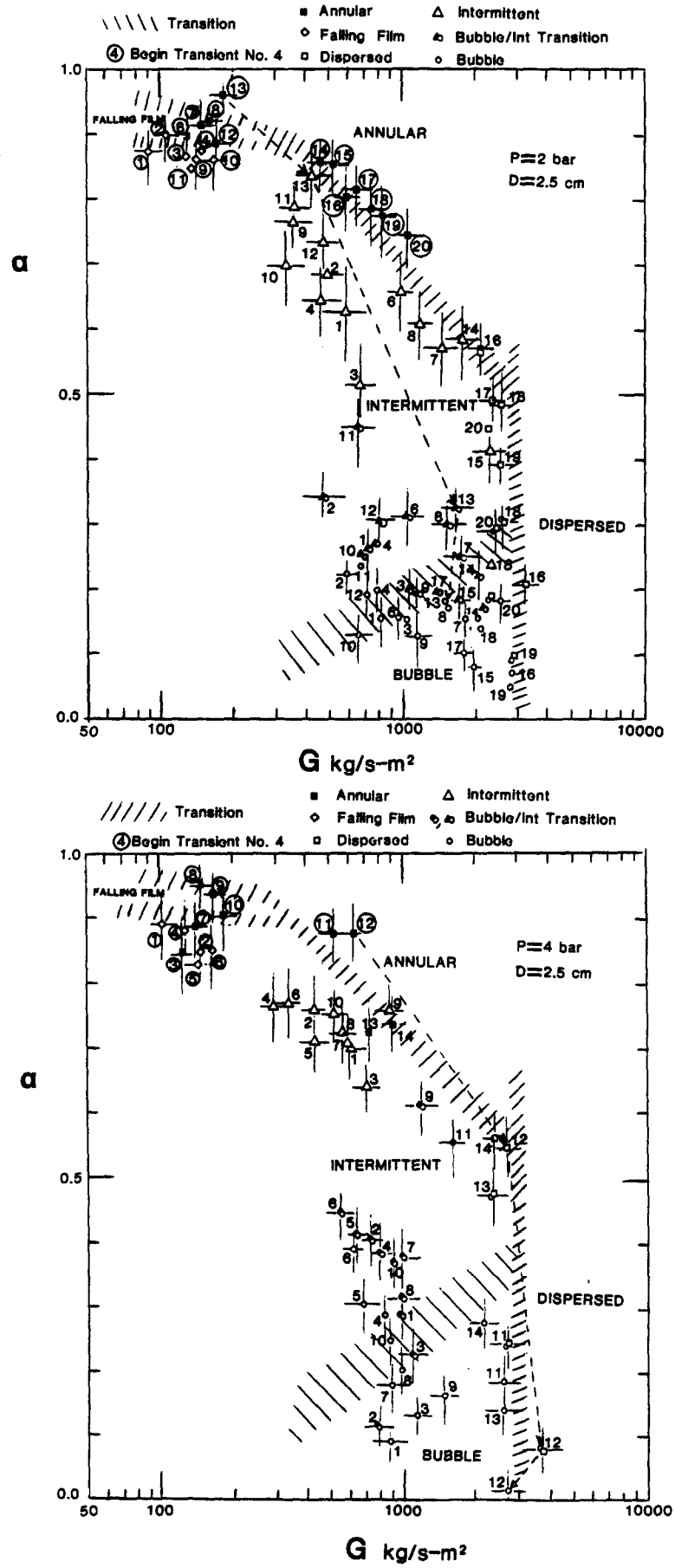

Figure 11. Annular/Intermittent/Bubble ($A/I/B$) flow transients. (a) $P = 2$ bar, (b) $P = 4$ bar.

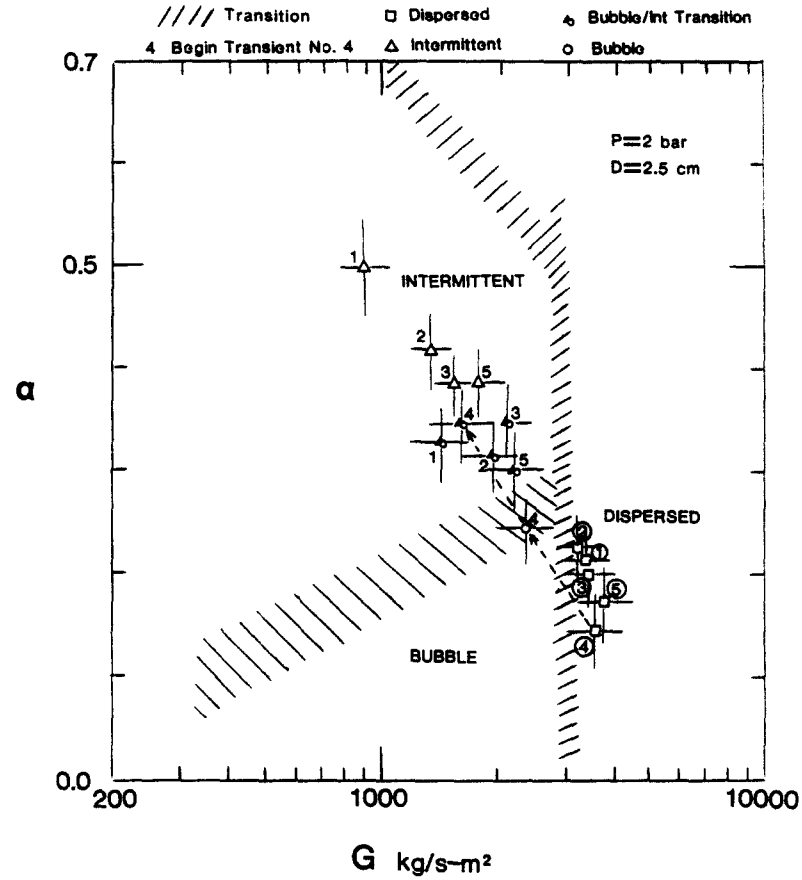

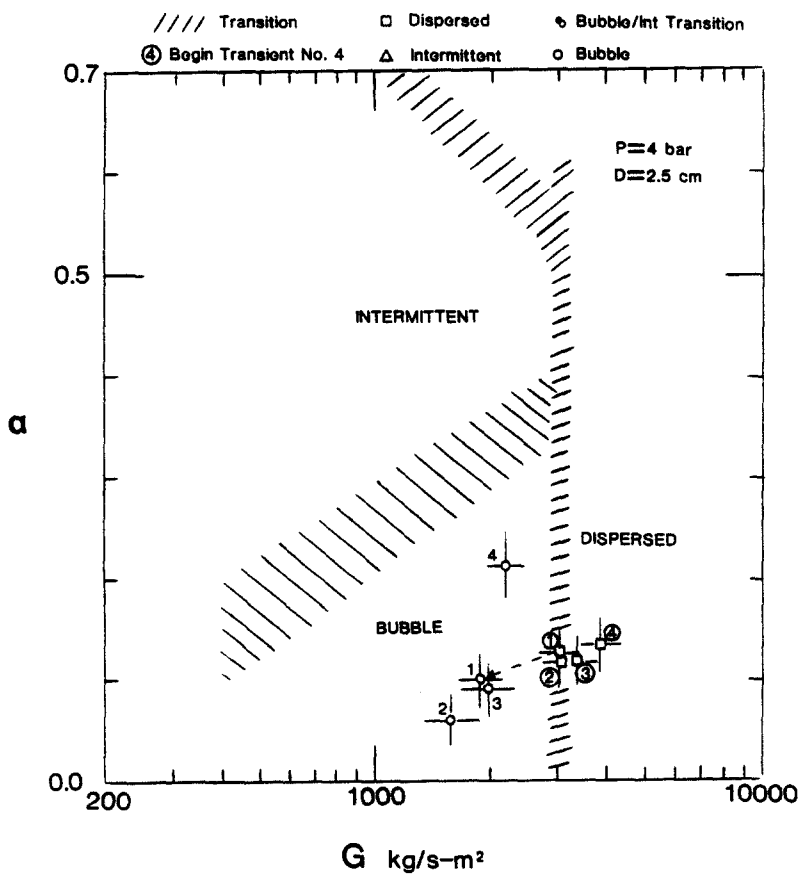

Figure 12. Dispersed/bubble/intermittent ($D/B/I$) flow transient. (a) $P = 2$ bar, (b) $P = 4$ bar.

various pressures. However, the steady-state map would seem to provide only an approximate guide for flow pattern transition behavior during flow transients in downflow. There appears to be a tendency for an existing flow pattern to persist somewhat past its steady-state boundaries. The only exception to this trend was the onset of dispersed flow which agreed with the steady-state transition boundary. The tendency for flow patterns to persist is not surprising since some finite time must be required to go from one structure to another.

The conclusions on downward flow pattern transition behavior during transients were arrived at by using the dynamic slip model for evaluating x from α. With the product $C_{LG}A_{LG}$ being taken as a unique function of α and G, it was found that the dynamic terms of the dynamic slip model were negligible for the present tests. Hence, the steady-state relationship between α and x could be used for the transients. if the product of $C_{LG}A_{LG}$ is not identical during the transient and steady-state for given values of α and G, then the computed mass velocities may be in error. That there may be some difference between steady-state and transient values of $C_{LG}A_{LG}$ is certainly possible since the transient and steady-state flow pattern maps were not identical. However, as may be seen from the plot of $C_{LG}A_{LG}$ in figure 3, there were no sharp changes in the value of $C_{LG}A_{LG}$ as the flow pattern changes. Hence, the persistance of a flow pattern would not be expected to lead to sharp deviations from the steady-state relationships.

In two of the transient categories, flow pattern transitions occured early in the transient. In the $A/I/B$ flow transients (figure 11) a number of the changes from annular or falling film to intermittent flow took place during the initial period when fluid quality was expected to remain constant since the fluid had left the heater prior to the onset of the transient. Similarly in the $D/B/I$ transients, some of the changes to bubble flow took place during the initial period. Calculation of the qualities from α for these points at the initial conditions and transition locations, using the steady-state α vs x relationships, indicated essentially constant quality as expected. This provides some confirmation of the procedure used for calculations of quality from α. It should be noted that these points, for which there was little doubt about the calculated quality, also showed the persistance of the original flow pattern somewhat beyond its steady-state boundary. Further studies of downward flow patterns during flow transients would be desirable in order to provide additional confidence in the present conclusions.

REFERENCES

BENNETT, A.W., HEWITT, G.F., KEARSEY, H.A., KEEYS, R.V.F. & LACEY, P.M.C. 1982 Flow visualization studies of boiling water at high pressure. Report No. AERE4874, Atomic Energy Research Establishment, Harwell, England; Collier, J.G., 1981 *Convective Boiling and Condensation*, 2nd ed., p. 16. McGraw-Hill, London.

CRAWFORD, T.J. 1983 Analysis of steady-state and transient two-phase flow in downwardly declined lines. Ph.D. thesis, Drexel University, Philadelphia, PA.

CRAWFORD, T.J., WEINBERGER, C.B. & WEISMAN, J. 1985 Two-phase flow pattern and void fractions in downward flow Part I: Steady-state flow patterns. *Int. J. Multiphase Flow* **11**, 761–782.

HUGHMARK, G.A. 1962 Holdup in gas–liquid flow. *Chem. Eng. Prog.* **58**, 62–65.

KAIZERMAN, S., WACHOLDER, E. & ELIAS, E. 1983 A drift flux model flow regime map of two-phase flows for thermal hydraulic calculators. *Nucl. Sci. Eng.* **84**, 166–167.

LAHEY, R.T. & MOODY, F.J. 1977 *The Thermal Hydraulics of a Boiling Water Nuclear Reactor*, p. 208. American Nuclear Society, LaGrange Park, Illinois.

MCFADDEN, J.H., PAULSEN, M.P. & GOSE, G.C. 1981 RETRAN dynamic slip model, *Nucl. Tech.* **54**, 287–297.

MISHIMA, K. & ISHI, M. 1984 Flow regime transition criteria for upward two-phase flow in vertical tubes. *Int. J. Heat Mass Transfer* **5**, 723–737.

PETRICK, M. 1963 A study of carry-under phenomena in vapor liquid separation. *AIChE J.* **9**, 253–260.

SAKAGUCHI, T., AKAGAWA, K. & HAMAGUSHI, H. 1976 Transient behavior of flow

patterns for air water two-phase flow in horizontal tubes. *Proceedings of the 26th Japanese National Conference on Applied Mechanics*, Vol. 26, unpublished.

SAKAGUCHI, T., AKAGAWA, K., HAMAGUCHI, H. & AMANO, T. 1979 Developing steady and transient air-water two-phase flow in horizontal tubes, in *Multiphase Transport Fundamentals, Reactor-Safety, Applications*, (Edited by T. N. Vezerogula), Vol.1. Hemisphere, Washington, D.C.

TAITEL, Y., LEE, N. & DUKLER, A.E. 1978 Transient gas–liquid flow in horizontal pipes: Modeling flow pattern transitions. *AIChE J.* **24**, 920–934.

TENTNER, A. 1977 An improved numerical analysis of transient two-phase flow phenomena using a slip model. Ph.D. Thesis, University of Cincinnati, Cincinnati, OH.

WEISMAN, J. 1977 Experimental data on two-phase pressure drop across area changes during flow transients. U.S. Nuclear Regulatory Commission Report No. NUREG-0306, Vol. 2, unpublished.

WEISMAN, J., DUNCAN, D., GIBSON, J., & CRAWFORD, T. 1979 Effects of liquid properties and pipe diameter on two-phase flow patterns in horizontal lines. *Int. J. Multiphase Flow* **5**, 437–462.

WEISMAN, J. & KANG, S.Y. 1981 Flow pattern transitions in vertical and upwardly inclined lines. *Int. J. Multiphase Flow* **7**, 271–291.

ZUBER, N. & FINDLAY, J. 1965 Average volumetric concentration in two-phase flow systems. *Trans. ASME, J.Heat Transfer* **87**, 453–459.